

pH dependence of the stability of barstar to chemical and thermal denaturation

RITU KHURANA, ANITA T. HATE, UTPAL NATH, AND JAYANT B. UDGAONKAR

National Centre for Biological Sciences, TIFR Centre, Indian Institute of Science Campus, Bangalore 560012, India

(RECEIVED January 19, 1995; ACCEPTED March 24, 1995)

Abstract

Equilibrium unfolding of barstar with guanidine hydrochloride (GdnHCl) and urea as denaturants as well as thermal unfolding have been carried out as a function of pH using fluorescence, far-UV and near-UV CD, and absorbance as probes. Both GdnHCl-induced and urea-induced denaturation studies at pH 7 show that barstar unfolds through a two-state $F \rightleftharpoons U$ mechanism and yields identical values for ΔG_U , the free energy difference between the fully folded (F) and unfolded (U) forms, of 5.0 ± 0.5 kcal·mol⁻¹ at 25 °C. Thermal denaturation of barstar also follows a two-state $F \rightleftharpoons U$ unfolding transition at pH 7, and the value of ΔG_U at 25 °C is similar to that obtained from chemical denaturation. The pH dependence of denaturation by GdnHCl is complex. The C_m value (midpoint of the unfolding transition) has been used as an index for stability in the pH range 2–10, because barstar does not unfold through a two-state transition on denaturation by GdnHCl at all pH values studied. Stability is maximum at pH 2–3, where barstar exists in a molten globule-like form that forms a large soluble oligomer. The stability decreases with an increase in pH to 5, the isoelectric pH of the protein. Above pH 5, the stability increases as the pH is raised to 7. Above pH 8, it again decreases as the pH is raised to 10. The decrease in stability from pH 7 to 5 in wild-type (*wt*) barstar, which is shown to be characterized by an apparent pK_a of 6.2 ± 0.2 , is not observed in H17Q, a His 17 → Gln 17 mutant form of barstar. This decrease in stability has therefore been correlated with the protonation of His 17 in barstar. The decrease in stability beyond pH 8 in *wt* barstar, which is characterized by an apparent pK_a of 9.2 ± 0.2 , is not detected in BSCCAA, the Cys 40 Cys 82 → Ala 40 Ala 82 double mutant form of barstar. Thus, this decrease in stability has been correlated with the deprotonation of at least one of the two cysteines present in *wt* barstar. The increase in stability from pH 5 to 3 is characterized by an apparent pK_a of 4.6 ± 0.2 for *wt* barstar and BSCCAA, which is similar to the apparent pK_a that characterizes the structural transition leading to the formation of the A form. The use of C_m as an index of stability has been supported by thermal denaturation studies. In the pH range where both chemical denaturation and thermal denaturation studies were possible, both C_m and T_m , the midpoint of a thermal denaturation curve displays similar trends. Very high pH (pH 12) is shown to completely unfold the protein in a fully reversible manner.

Keywords: acid denaturation; base denaturation; molten globules; protein folding; protein stability

The importance of electrostatic interactions in determining the stability of a protein has long been recognized (Tanford, 1970). The roles and magnitudes of specific electrostatic interactions in a protein can be studied by measuring the dependence of the stability on pH, or by perturbing the interaction through site-directed mutagenesis. pH is known to influence the stability of

a protein by altering the net charge on the protein, and many proteins denature at extremes of pH because of the presence of destabilizing repulsive interactions between like charges (Linderström-Lang, 1924). Alternatively, if a titratable group is buried in an un-ionized form in the interior of the protein and can be titrated only upon unfolding, the unfolded state will be favored upon titration of the group by changing the pH (Beychok & Steinhardt, 1959). The pH dependence of protein stability needs to be explained on the basis of the coupling of the protonation reactions that occur on changing pH with the unfolding reaction, with the unfolded and folded states binding protons to different extents (Hermans & Scheraga, 1961; McPhie, 1975; Sali et al., 1988; Anderson et al., 1990).

Extremes of pH do not always completely denature a protein but may lead to only partly folded states (Fink et al., 1994), commonly referred to as molten globules. Molten globule-like forms

Reprint requests to: Jayant Udgaonkar, National Centre for Biological Sciences, TIFR Centre, P.O. Box 1234, Indian Institute of Science Campus, Bangalore 560012, India; e-mail: jayant@tifrbng.ernet.in; jayant@tifrvax.tifr.res.in.

Abbreviations: BSCCAA, a Cys 40 Cys 82 → Ala 40 Ala 82 double mutant form of barstar; H17Q, a His 17 → Gln 17 mutant form of barstar; F , fully folded form of barstar at pH 7–8; F^- , the F form with at least one deprotonated cysteine side chain; F^+ , the F form with His 17 protonated; A , molten globule-like form of barstar; D , base-denatured form of barstar; S , Svedberg (unit of sedimentation coefficient).

of proteins have evinced much attention in recent years because they appear to resemble kinetic folding intermediates (Kuwajima, 1992). Unlike kinetic intermediates, molten globule-like forms are amenable to detailed structural characterization (Alexandrescu et al., 1993; Redfield et al., 1994) because they are structures that exist at equilibrium.

Barstar, the intracellular inhibitor to barnase in *Bacillus amyloliquefaciens* is an attractive model protein for the study of protein folding (Hartley, 1988). The X-ray crystal structure of the complex of barnase and BSCCAA, a Cys 40 Cys 82 → Ala 40 Ala 82 double mutant form of barstar has been solved and shows that barstar is comprised of four α -helices and a parallel three-stranded β -sheet (Guillet et al., 1993). This has been confirmed by the solution structure of wild-type (*wt*) barstar (Lubienski et al., 1994). Kinetic studies of both BSCCAA (Schreiber & Fersht, 1993a) and *wt* barstar (Shastry et al., 1994) have provided evidence for the presence of multiple folding intermediates and at least three parallel folding pathways. Both *wt* barstar (Khurana & Udgaonkar, 1994) and BSCCAA (Swaminathan et al., 1994) transform into molten globule-like conformations at low pH. The use of ANS binding to monitor the folding kinetics of barstar has revealed the presence of two, very early, molten globule-like intermediates on the kinetic folding pathways (Shastry & Udgaonkar, 1995), but the relationship between these kinetic intermediates and the equilibrium intermediate that forms at low pH is yet to be established.

In this paper, the pH dependence of the stability has been characterized by chemical denaturant-induced unfolding studies as well as by thermally induced unfolding studies over the pH range 2–10. Of specific interest has been the pH range 7–8, where the binding of barstar to barnase is tightest (Schreiber & Fersht, 1993b). Even relatively minor deviations from these pH values seem to have a significant effect on the stability of barstar. It is shown here that the stability of the protein is not maximal at the isoelectric point (pH 5), as theoretically predicted (Linderström-Lang, 1924), and as actually observed in the case of ribonuclease T1 and ribonuclease A (Pace et al., 1990). Some of the interactions that are affected by a change in pH have been identified by examining the pH profiles of the stabilities of two mutant forms of barstar, BSCCAA and H17Q. The roles of the two cysteine residues and of the sole histidine residue in determining the pH dependence of the stability of barstar have been established.

Results

Figures 1 and 2 show equilibrium denaturation curves obtained for barstar at pH 7, 25 °C, using GdnHCl and urea as the denaturants, respectively. In either case, both fluorescence and far-UV CD gave completely superimposable denaturation curves (Figs. 1C, 2C). The data in Figures 1 and 2 have therefore been fit to a two-state $F \rightleftharpoons U$ model for unfolding using Equations 1, 2, and 3. The free energy for unfolding in the absence of denaturant was obtained by linear extrapolation of the $\Delta G_U(D)$ to zero denaturant concentration. The values obtained for $\Delta G_U(\text{H}_2\text{O})$ from the GdnHCl and urea denaturation curves were identical within experimental error and are given in the legends to Figures 1 and 2. The values obtained for C_m (2.0 ± 0.1 M for GdnHCl and 4.7 ± 0.2 M for urea) obtained using far-UV CD as the probe for unfolding match the values reported earlier with fluorescence as the probe for unfolding (Khurana &

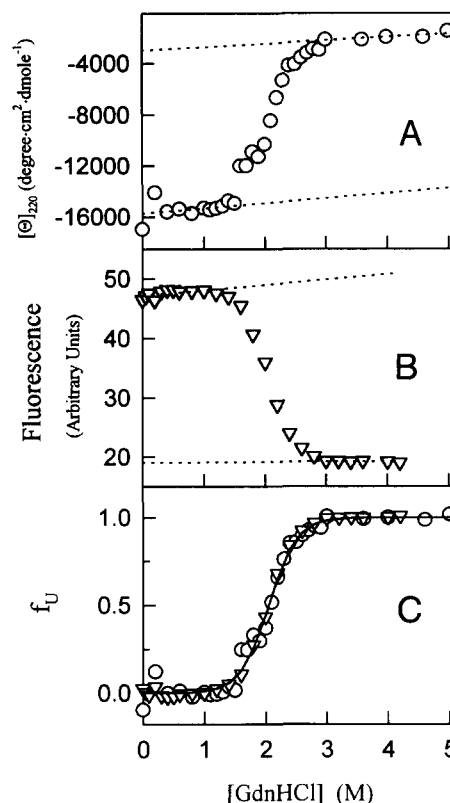


Fig. 1. GdnHCl-induced denaturation of *wt* barstar at pH 7, 25 °C. Denaturation was monitored by measurement of (A) mean residue ellipticity at 220 nm and (B) fluorescence at 322 nm on excitation at 287 nm. Dashed lines in A and B are least-squares fits of the folded and unfolded baselines to straight lines. Data in A and B were converted to f_U using Equation 1, and a plot of f_U versus GdnHCl concentration is shown in C. Solid line in C is a nonlinear least-squares fit of the data to Equations 2 and 3 and yields $\Delta G_U = 5.2 \pm 0.5$ kcal·mol⁻¹ and $m_G = -2.5 \pm 0.4$ kcal·mol⁻¹ M⁻¹.

Udgaonkar, 1994). Similarly, it has been shown that BSCCAA unfolds by a two-state $F \rightleftharpoons U$ transition between pH 6 and 9 (Fig. 9). The value obtained for ΔG_U for the unfolding of BSCCAA, 4.4 kcal·mol⁻¹, is similar to the value of 4.8 kcal·mol⁻¹ reported earlier (Schreiber & Fersht, 1993a).

In Figure 3 are shown thermal denaturation curves obtained for barstar at pH 7, using three different optical probes (far-UV CD, near-UV CD, and absorbance at 287 nm) to monitor unfolding. All three probes yield superimposable thermal transitions, characterized by identical midpoints of the transition, T_m , of 71.5 ± 0.5 °C. The data were therefore analyzed according to a two-state $F \rightleftharpoons U$ model for unfolding using Equations 4, 5, and 6. The value obtained for the enthalpy change, ΔH_m , at T_m , is 60 ± 5 kcal·mol⁻¹. A van't Hoff analysis of the data also yields a similar value for ΔH_m of 60 ± 5 kcal·mol⁻¹.

Determination of ΔC_p

Thermal denaturation curves were determined at pH 7 in the presence of different concentrations of GdnHCl in the range 0.2–1.3 M. T_m decreases with an increase in GdnHCl concen-

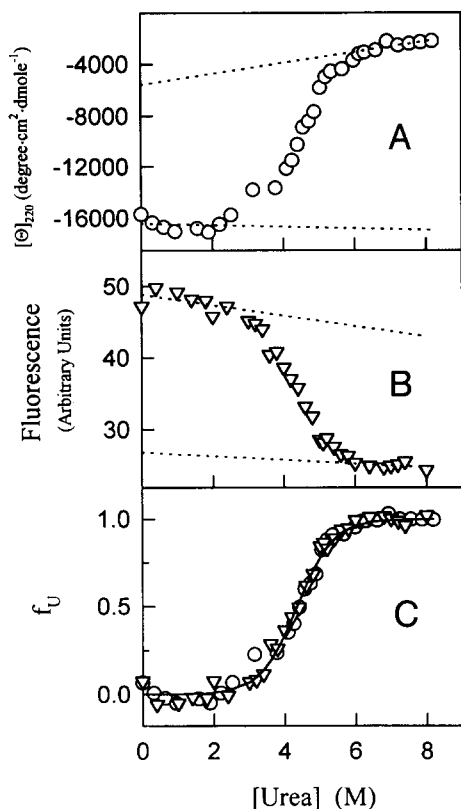


Fig. 2. Urea-induced denaturation of *wt* barstar at pH 7, 25 °C. Denaturation was monitored by measurement of (A) mean residue ellipticity at 220 nm or (B) fluorescence at 322 nm on excitation at 287 nm. Dashed lines in A and B are least-squares fits of the folded and unfolded baselines to straight lines. Data in A and B were converted to f_U using Equation 1, and a plot of f_U versus urea concentration is shown in C. Solid line in C is nonlinear least-squares fit of the data to Equations 2 and 3 and yields $\Delta G_U = 5.0 \pm 0.5$ kcal·mol⁻¹ and $m_G = -1.2 \pm 0.2$ kcal·mol⁻¹·M⁻¹.

tration from 71.5 ± 0.5 °C in the absence of GdnHCl to 55.0 ± 0.5 °C in the presence of 1.3 M GdnHCl. The value of ΔH_m was determined at each value of T_m using Equations 4, 5, and 6. In Figures 4A and B, ΔH_m is plotted against T_m for *wt* barstar at pH 7 and BSCCAA at pH 8, respectively. The slopes of the straight lines through the data yield, according to the Kirchoff equation, values for ΔC_p of 1.2 ± 0.25 kcal·mol⁻¹·K⁻¹ for *wt* barstar at pH 7 (Fig. 4A) and 1.3 ± 0.3 kcal·mol⁻¹·K⁻¹ for BSCCAA at pH 8 (Fig. 4B).

Test of the linear free energy model

Once the value of ΔC_p was determined, it was possible to determine ΔG_U at 25 °C by the use of Equation 4, both in the absence and in the presence of different concentrations of GdnHCl. In the absence of GdnHCl at pH 7, the value of ΔG_U at 25 °C for *wt* barstar was determined to be 5.4 ± 0.5 kcal·mol⁻¹, which is similar to the value for ΔG_U at 25 °C obtained by denaturant unfolding (see above). In Figure 5, the values of ΔG_U at 25 °C similarly determined in the presence of different concentrations of GdnHCl in the range 0–1.3 M are plotted against GdnHCl concentration for both *wt* barstar and BSCCAA. Also included are values for ΔG_U obtained from the transition zones of GdnHCl-induced denaturation curves such as that shown for *wt* barstar in Figure 1. It is seen that there is a linear dependence of ΔG_U on GdnHCl concentration in the range 0–2.4 M. The straight line through the data for either *wt* barstar or BSCCAA extrapolates linearly to a value for ΔG_U (H₂O), similar to that determined from the thermal denaturation curve obtained in the absence of GdnHCl. The slope of the straight line for *wt* barstar in Figure 5A is -2.6 ± 0.4 kcal·mol⁻¹·M⁻¹, which corresponds to the value of m_G obtained from the GdnHCl-induced transition shown in Figure 1. The m_G value obtained for BSCCAA from Figure 5B is -2.0 ± 0.4 kcal·mol⁻¹·M⁻¹.

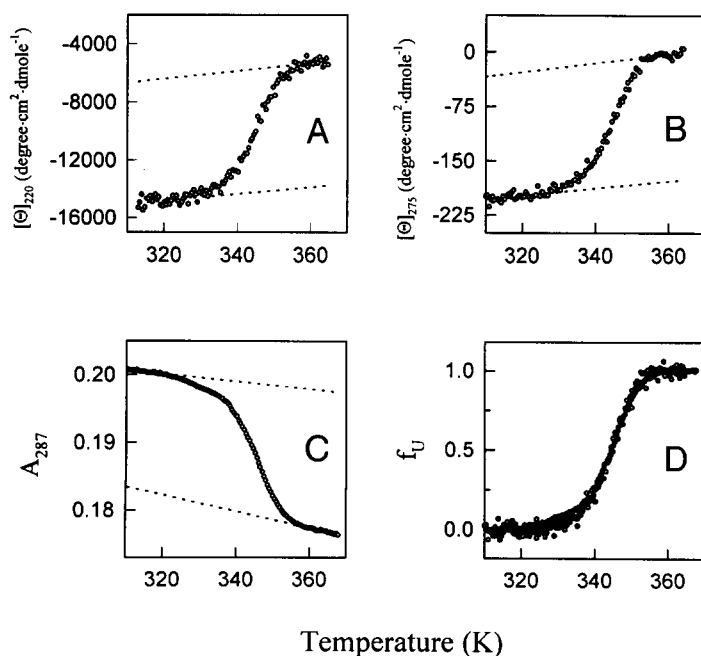


Fig. 3. Thermal denaturation of *wt* barstar at pH 7. Thermal denaturation was followed by (A) CD at 220 nm, (B) CD at 275 nm, and (C) absorbance at 287 nm. Concentrations of barstar were 5 μ M, 50 μ M, and 10 μ M, respectively. Dashed lines in A, B, and C are linear least-squares fits of the folded and unfolded baselines to straight lines. The data in A, B, and C were converted to f_U according to Equation 1 and a plot of f_U is shown in D. The solid line through the data in D is drawn according to Equation 7, with the values of ΔH_m (60 kcal·mol⁻¹) and T_m (71.5 °C) determined using Equations 4, 5, and 6, and with the value of ΔC_p fixed to the value obtained (1.2 kcal·mol⁻¹·K⁻¹) in Figure 4A.

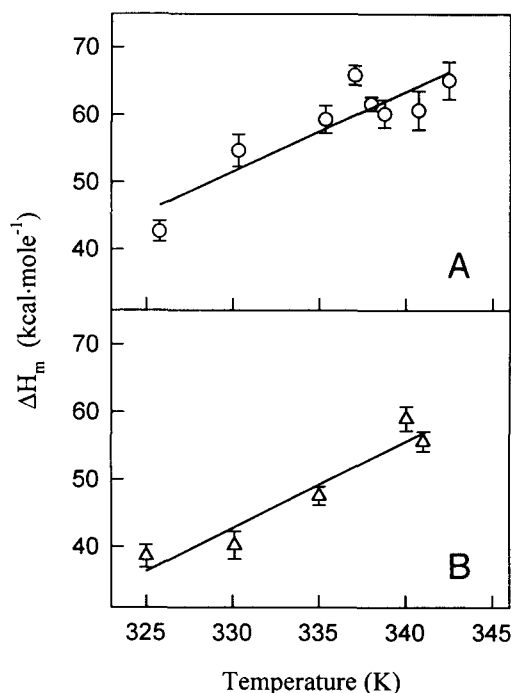


Fig. 4. Determination of ΔC_p . Thermal denaturation experiments were performed in the presence of different concentrations of GdnHCl at (A) pH 7 for *wt* barstar and (B) pH 8 for BSCCAA, to vary T_m . ΔH_m was determined at each value of T_m from the slope of the van't Hoff plot. Straight lines through the data are linear least-squares fits to the data, and yield values for ΔC_p of $1.2 \pm 0.25 \text{ kcal}\cdot\text{mol}^{-1}\cdot\text{K}^{-1}$ (*wt* barstar) and $1.3 \pm 0.3 \text{ kcal}\cdot\text{mol}^{-1}\cdot\text{K}^{-1}$ (BSCCAA).

Determination of the size of the A form and the N state for barstar

Both sedimentation equilibrium experiments and gel-filtration experiments show that barstar exists as a monomer at pH 7 (data not shown). Sedimentation velocity experiments indicate that the A form at pH 3 exists as a large soluble oligomer: it has an *S* value of 7.9 compared to the *S* value of 1.3 for the N state.

Unfolding of barstar at high pH

Barstar unfolds at high pH (beyond pH 10). In Figure 6A, the unfolding at high pH has been demonstrated by measurement of the loss in secondary structure as monitored by far-UV CD. The mean residue ellipticity at 220 nm of the protein at pH 12 is $-2,800 \pm 300 \text{ degree}\cdot\text{cm}^2\cdot\text{dmol}^{-1}$, which is similar to the value ($-2600 \text{ degree}\cdot\text{cm}^2\cdot\text{dmol}^{-1}$) expected for a random coil conformation of a polypeptide chain (Chen et al., 1972), but which is more than the value reported ($-1,600 \text{ degree}\cdot\text{cm}^2\cdot\text{dmol}^{-1}$) for *wt* barstar in 6 M GdnHCl at pH 7 (Khurana & Udgaonkar, 1994). In Figure 6B, the loss in tertiary structure upon high pH unfolding has been monitored by following the loss in fluorescence intensity at 337 nm. In Figure 6C, the base-induced unfolding reaction has been monitored by following the increase in the wavelength of maximum fluorescence emission. The wavelength of maximum fluorescence emission increases from 337 nm at pH values between 7 and 9, where the protein is in the fully folded *F* state, to 356 nm at pH 12, where the protein is in the

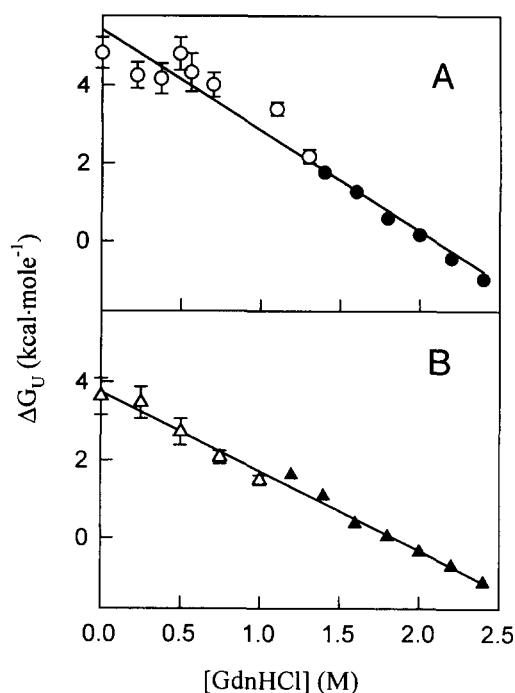


Fig. 5. Linear dependence of ΔG_U on GdnHCl concentration at 25 °C. **A:** *wt* barstar at pH 7. **B:** BSCCAA at pH 8. Thermal denaturation curves were obtained in the presence of 0.2–1.3 M GdnHCl, and the value of ΔG_U at 25 °C was determined in each case (open symbols) from the use of Equations 4, 5, and 6, and the values for ΔC_p of $1.2 \text{ kcal}\cdot\text{mol}^{-1}\cdot\text{K}^{-1}$ (*wt* barstar) and $1.3 \text{ kcal}\cdot\text{mol}^{-1}\cdot\text{K}^{-1}$ (BSCCAA) were determined from Figure 4. Closed symbols are the values of ΔG_U obtained from GdnHCl-induced denaturation curves as shown for *wt* barstar in Figure 1. Solid lines through the data are linear least-squares fits to the data and have slopes of $-2.6 \pm 0.4 \text{ kcal}\cdot\text{mol}^{-1} \text{ M}^{-1}$ (*wt* barstar) and $-2.2 \pm 0.4 \text{ kcal}\cdot\text{mol}^{-1} \text{ M}^{-1}$ (BSCCAA).

fully unfolded *D* form. The wavelength of maximum emission of barstar in 6 M GdnHCl at pH 7 is also 356 nm, indicating that barstar is indeed completely unfolded at pH 12. It should be noted that there was an error of 5 nm in values reported earlier (Khurana & Udgaonkar, 1994) for the wavelengths of maximum fluorescence emission at pH 7 both in the absence (332 nm) and presence of 6 M GdnHCl (351 nm) because of an error in the calibration of the fluorimeter used. The data in Figure 6 indicate that base-induced unfolding commences only above pH 10. Moreover, this unfolding reaction is completely reversible. Not only is the entire fluorescence signal restored when protein at pH 12 is returned to pH 7, but so is the activity (data not shown). Fits of all three data sets in Figure 6 to Equation 8 yield a value for pH_{m1} , the midpoint of the unfolding transition, of 11.0 ± 0.1 .

pH dependence of C_m

Equilibrium denaturation curves were obtained in the pH range 2–10 at 25 °C, using both fluorescence at 322 nm and mean residue ellipticity at 220 nm as probes for GdnHCl-induced unfolding, for *wt* barstar, BSCCAA, and H17Q. The midpoint of the unfolding transition, C_m , is plotted against pH in Figure 7A for *wt* barstar, Figure 7B for BSCCAA, and Figure 7C for H17Q. The C_m value has been used as a measure of stability through-

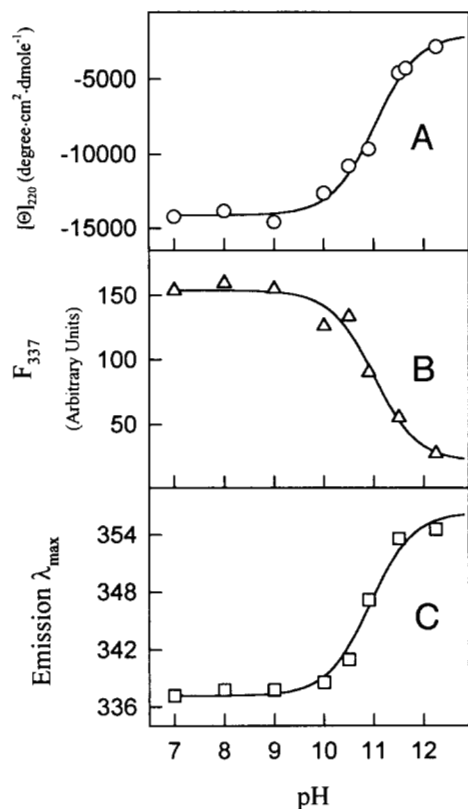


Fig. 6. Base-induced unfolding of *wt* barstar at 25 °C. Unfolding was followed by monitoring the pH dependence of (A) mean residue ellipticity at 220 nm, (B) fluorescence intensity at 337 nm, and (C) wavelength of maximum fluorescence emission. Solid lines through the data are nonlinear least-squares fits to Equation 8. All three curves yield an identical value of 11.0 ± 0.1 for the apparent pK_a (pH_{m1}) that characterizes the unfolding transition.

out the pH range as ΔG_U could not be determined because of the three-state unfolding that is observed at lower pH values (Khurana & Udgaonkar, 1994).

At pH 5, C_m is lower than at pH 7 when determined from both fluorescence- and mean residue ellipticity-monitored denaturation curves for *wt* barstar. For BSCCAA, C_m , whether determined from fluorescence or mean residue ellipticity-monitored denaturation curves, has a minimum value at pH 4.8. Also, for both *wt* barstar and BSCCAA, it is seen that fluorescence-monitored unfolding precedes far-UV CD-monitored unfolding in the pH range 2–5. Both probes yield superimposable denaturation transition curves between pH 7 and 9 for *wt* barstar and above pH 6 for BSCCAA. Thus, folding can be described by a two-state $F \rightleftharpoons U$ model for unfolding between pH 7 and 9 for *wt* barstar and above pH 6 for BSCCAA, but below pH 6, at least one equilibrium folding intermediate, *I*, accumulates and folding must be described by a three-state $F \rightleftharpoons I \rightleftharpoons U$ model for unfolding. For H17Q, the two-state model for unfolding is not valid at any pH and even at pH 7 at least one intermediate is involved in the unfolding of this protein (Nath & Udgaonkar, 1995). The unfolding of H17Q follows a three-state $F \rightleftharpoons I \rightleftharpoons U$ unfolding model at all pH values.

The increase in the C_m values for GdnHCl-induced unfolding of *wt* barstar from pH 5 to 3 is characterized by a pH_{m4}

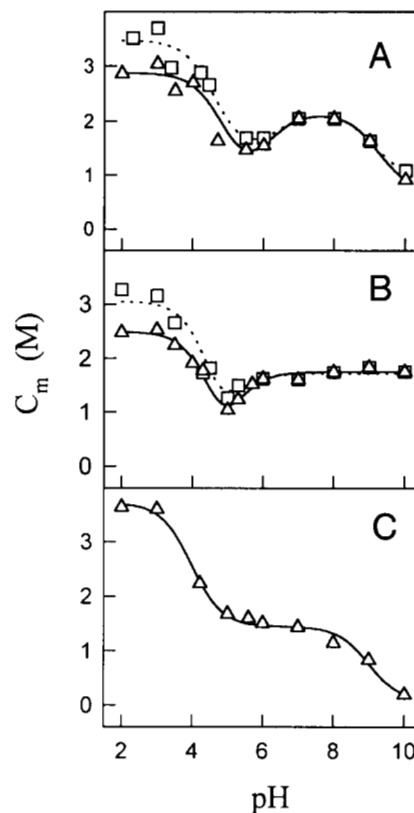


Fig. 7. pH dependence of C_m at 25 °C for (A) *wt* barstar, (B) BSCCAA, and (C) H17Q. GdnHCl-induced equilibrium denaturation curves were obtained at the pH values shown, using both fluorescence at 322 nm on excitation at 287 nm (Δ) and mean residue ellipticity at 220 nm (\square) as the probes for unfolding. The C_m value for each curve was obtained as the midpoint of the GdnHCl concentration at which the protein is half unfolded. For *wt* barstar, the solid line through the fluorescence data and the dashed line through the CD data are nonlinear least-squares fits to Equation 9 and yield values for pH_{m2} , pH_{m3} , and pH_{m4} of 9.2 ± 0.2 , 6.2 ± 0.2 , and 4.6 ± 0.2 , respectively. For BSCCAA, the solid line through the fluorescence data and the dashed line through the CD data are nonlinear least-squares fits to Equation 10 and yield values for pH_{m3} and pH_{m4} of 5.0 ± 0.2 and 4.6 ± 0.2 , respectively. For H17Q, the solid line through the fluorescence data is a nonlinear least-squares fit to Equation 11 and yields values for pH_{m2} and pH_{m4} of 9.2 ± 0.2 and 4.0 ± 0.2 , respectively. The C_m value at pH 10 for H17Q was determined by inspection only because a good native baseline could not be obtained for the GdnHCl-induced unfolding transition.

(Equation 9) value of 4.6 ± 0.2 , which also represents the apparent pK_a value that characterizes the structural change leading to the formation of an alternative conformation (*A* form) having molten globule-like properties (Khurana & Udgaonkar, 1994). This increase in C_m at low pH is characterized by similar apparent pK_a value for BSCCAA but for H17Q this value is 4.0 ± 0.2 , which is significantly lower than the *wt* value. For *wt* barstar and H17Q, there is a decrease in the value of C_m above pH 8, which is characterized by an apparent pK_a value (pH_{m2} in Equation 9) of 9.2 ± 0.2 . This decrease in stability at high pH is not seen for BSCCAA. Again a decrease in the value of C_m is observed from pH 7 to 5 in the case of *wt* barstar and is characterized by an apparent pK_a value (pH_{m3} in Equation 9) of 6.2 ± 0.2 . A similar decrease in stability is also observed from pH 6 to 5 in the case of BSCCAA, but no such decrease

is seen in the case of H17Q. The apparent pK_a value (pH_{m3} in Equation 10) for this transition for BSCCAA is 5.0 ± 0.2 , which is significantly lower than the apparent pK_a value observed for *wt* barstar.

pH dependence of T_m

The midpoint of the thermally induced unfolding transition, T_m , is plotted versus pH in Figure 8 for *wt* barstar, BSCCAA, and H17Q. T_m decreases with increasing pH in the range 7–10 for both *wt* barstar and H17Q with a similar slope and this decrease is negligible in the case of BSCCAA. The number of protons released from the native state of protein on increasing the pH to 9, $\Delta_m v$, as determined by Equation 12 (see Materials and methods) is 0.7 for *wt* barstar and is only 0.3 for BSCCAA. There is also a decrease in the value of T_m between pH 6 to 5 in the case of both *wt* barstar and BSCCAA, which is not observed in the case of H17Q. Equation 12 could not be used to determine the value of $\Delta_m v$ for this transition between the F and F^+ forms because the thermal unfolding transition in this pH range is not two state, and consequently, Equations 7 and 8 could not be used to determine ΔH_m . It was not possible to determine values for T_m below pH 5, because the A form that is populated at low pH values does not undergo any thermal unfolding transition up to 98 °C (Khurana & Udgaonkar, 1994).

pH dependence of ΔG_U

ΔG_U has been determined only in the pH range where two-state unfolding transitions are observed. The decrease in stability of *wt* barstar on increasing the pH from 7 to 9 is also reflected in the decrease in the value of ΔG_U , as shown in Figure 9. For BSCCAA, ΔG_U does not change at all from pH 6 to 10. At all other pH values ΔG_U could not be determined because both *wt* barstar and BSCCAA follow three-state unfolding transitions. Analysis according to a three-state $F \rightleftharpoons I \rightleftharpoons U$ model (Nath & Udgaonkar, 1995) was not attempted because the optical properties of the intermediate I are not known.

ANS binding experiments

ANS (10 μ M) was added to barstar (2 μ M) both in the absence of GdnHCl and in the presence of different concentrations of GdnHCl in the folding transition zone at pH 5.5. In no case was there any increase in fluorescence at 480 nm on excitation at 380 nm, indicating that the folding intermediate that is populated in the folding transition zone at pH 5.5 does not have hydrated hydrophobic surfaces to which ANS can bind. Similarly, no ANS binding was observed at both pH 10 and pH 12, in the presence as well as in the absence of 0.2 M KCl, indicating that molten globule-like conformations do not accumulate at these pH values.

Discussion

Tests of the linear free energy model

The linear free energy model (Schellman, 1978) is widely used to determine the value of the free energy of unfolding in water, ΔG_U , from urea- and GdnHCl-induced unfolding curves. The validity of this model for the folding of *wt* barstar and BSCCAA

has been tested in three different ways. (1) Both urea and GdnHCl-induced denaturation curves yield identical values for ΔG_U in water at pH 7 (Figs. 1, 2), when Equation 3 was used to linearly extrapolate to ΔG_U at zero denaturant concentration. (2) The value so obtained for ΔG_U in the absence of denaturant from chemical denaturation studies is similar to the value obtained from thermal denaturation studies. (3) Thermal denaturation curves obtained in a range of GdnHCl concentrations in the pretransition zone (between 0.2 and 1.3 M GdnHCl) yield values for ΔG_U in the presence of these concentrations of GdnHCl. These values agree well with the values obtained from a linear extrapolation from the folding transition zone between 1.3 and 2.4 M GdnHCl (Fig. 5). This confirms the linear dependence of ΔG_U on GdnHCl concentration in the pretransition zone (Pace & Laurents, 1989). Moreover, the values obtained for m_G for both *wt* barstar (Fig. 5A) and BSCCAA (Fig. 5B) from the dependence of ΔG_U over the entire range of GdnHCl concentrations (0–2.4 M) are similar to the values obtained for these proteins using GdnHCl concentrations only in the folding transition zone, as illustrated in Figure 1 for *wt* barstar. Thus, the data in Figures 1, 2, 3, 4, and 5 validate the use of the linear free energy model to analyze unfolding of barstar by chemical denaturants.

Acid denaturation

It has been previously shown (Khurana & Udgaonkar, 1994) that acid denaturation of barstar, like that of other proteins including apomyoglobin (Griko et al., 1988), bovine carbonic anhydrase (Dolgikh et al., 1983), and retinol binding protein (Bychkova et al., 1992), leads to the formation of the partly folded A form, which resembles a molten globule. Here, sedimentation velocity measurements have been utilized to show that the A form of barstar exists as a large soluble oligomer with an apparent molecular weight of approximately 150,000. The formation of the soluble oligomer is probably because of hydrophobic interactions between the hydrated hydrophobic residues of different monomers and is presumably the reason why the A form of barstar at pH 3 is apparently more stable to chemical denaturation than the functional F state at pH 7.

The unfolding of the A form by chemical denaturants was also reported to occur through an $A \rightleftharpoons I_A \rightleftharpoons U$ mechanism (Khurana & Udgaonkar, 1994), where I_A is one or a collection of intermediates. It became important to determine whether the unfolding of the oligomeric A form with increasing denaturant concentration was proceeding first by dissociation of the oligomer to monomers, and then by subsequent unfolding of the A form monomers with a further increase in denaturant concentration. Such an unfolding mechanism has been observed for several oligomeric proteins, including aspartate aminotransferase (Herold & Kirchner, 1990) and *trp* aporepressor (Eftink et al., 1994). To test whether I_A , which is populated in the folding transition zone, corresponds to a monomeric A form, gel-filtration studies of barstar were carried out in the presence of different concentrations of GdnHCl in the pretransition and folding transition zones. In the presence of any concentration of GdnHCl in this range, the soluble oligomer, which eluted in the void volume, and the U state were the only two forms of the protein observed (data not shown). It therefore appears that dissociation of the oligomeric A form occurs simultaneously with unfolding to the U state. Although the A form exists as a large

oligomer, the two-dimensional proton NMR spectrum of the protein reveals a considerable amount of structure (S. Ramachandran & J.B. Udgaonkar, unpubl. results), the analysis of which is now in progress. The NMR structures of the molten globule-like forms of α -lactalbumin (Alexandrescu et al., 1993) and interleukin-4 (Redfield et al., 1994) show that stable localized secondary structures are preserved, mainly in the hydrophobic core region of the protein, and exposed regions have largely disordered structures.

Base denaturation

The data in Figure 6 show that *wt* barstar does not undergo any structural transition, as monitored by far-UV CD and fluorescence, in the pH range 6–10. On a further increase in pH, the protein unfolds reversibly to a base-denatured form, referred to here as the *D* form. Figure 6 shows that the *D* form is completely unfolded. The mean residue ellipticity at 220 nm for the *D* form is similar to that expected for a random coil (see Results), and the wavelength of maximum fluorescence emission is the same as that for the protein in 6 M GdnHCl, indicating that the tryptophan residues in the *D* form are as completely solvent exposed as in the *U* form. In the case of several proteins, including bovine and human α -lactalbumin (Robbins & Holmes, 1970; Dolgikh et al., 1981), β -lactamase (Goto & Fink, 1989; Goto et al., 1990), horse cytochrome *c* (Ohgushi & Wada, 1983), bovine growth hormone (Burger et al., 1966), and colicin A (Cavard et al., 1988), it has been reported that the fully unfolded form that is formed at an extreme of pH becomes molten globule-like under high ionic strength conditions. The *D* form of barstar does not, however, appear to become molten globule-like under high ionic strength conditions, as determined by its inability to bind ANS under these conditions (see Results). The value of 11.0 for the apparent pK_a that characterizes the base denaturation reaction (Fig. 6) points to the involvement of the deprotonation of the side chain of a *Tyr* or *Lys* residue.

pH dependence of stability below pH 7

On decreasing the pH from 7, there is first a decrease in stability of *wt* barstar from pH 7 to pH 5 that is characterized by an apparent pK_a of 6.2 ± 0.2 (Fig. 7A). The value for the apparent pK_a is near the intrinsic pK_a value (7.0) of His, suggesting that the decrease in stability may be a consequence of protonation of the His residue. *wt* barstar has a single His residue. To confirm that protonation of this residue is involved in the decrease in stability between pH 7 and 5, the pH dependence of the stability of H17Q, in which the sole His residue in barstar was mutated to Gln, was studied. The decrease in stability between pH 7 and 5 is not observed in the case of H17Q (Fig. 7C). Thus, protonation of His 17 is responsible for the decrease in stability as the pH is decreased from pH 7 to 5. A similar decrease in stability below pH 7 has also been observed in the case of T4 lysozyme (Anderson et al., 1990) and barnase (Sali et al., 1988; Pace et al., 1992), and in both of these proteins, the decrease in stability below pH 7 has been shown to be due to the protonation of a His residue.

The decrease in stability from pH 7 to pH 5 is also seen, as expected, for BSCCAA (Fig. 7B). The apparent pK_a for the same transition in BSCCAA, which has a value of 5.0 ± 0.2 , is,

however, significantly lower than that for *wt* barstar. The reason for this lower value for BSCCAA for the same transition is not understood. The decrease in stability from pH 7 to pH 5, as monitored by a decrease in the value of C_m , the midpoint of a GdnHCl-induced denaturation curve, has also been confirmed by measurement of the pH dependence of the value of T_m , the midpoint of a thermally induced denaturation curve. As seen in Figure 8, T_m decreases from pH 7 to pH 5 in the case of both *wt* barstar and BSCCAA, but not for H17Q.

On further lowering the pH, there is an increase in stability as reflected in the increase in the value of C_m for *wt* barstar as well as for BSCCAA. This increase in stability is characterized by an apparent pK_a value of 4.6 ± 0.2 (Fig. 7A,B). This value for the apparent pK_a is the same as the value of the apparent pK_a that characterizes the structural unfolding transition leading to the formation of the *A* form, as monitored by measurement of the mean residue ellipticity at 220 nm or the fluorescence at 322 nm (Khurana & Udgaonkar, 1994). This increase in stability is also seen for H17Q, but the value of the apparent pK_a (4.0 ± 0.2) that characterizes this increase in stability for the same transition is significantly lower than the *wt* pK_a . The value of the apparent pK_a characterizing the transition to the *A* form is

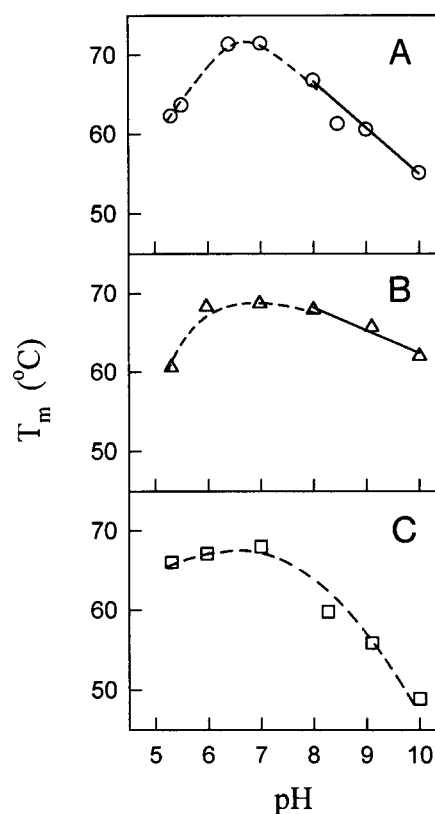


Fig. 8. pH dependence of T_m . Thermally induced equilibrium denaturation curves were obtained at the pH values shown for (A) *wt* barstar, (B) BSCCAA, and (C) H17Q using mean residue ellipticity at 220 nm as the probe for unfolding. The T_m value for each curve was obtained as the temperature at which the protein is half unfolded. Dashed lines through the data are drawn by inspection only. Solid lines indicate slopes of the individual high pH transitions at pH 9. These slopes are used in Equation 12 to obtain the number of protons released from the native state in the transition between pH 8 and 10.

close to the intrinsic pK_a values of Asp and Glu residues, indicating that the transition may be coupled to the protonation of one or more of the Asp or Glu residues in barstar.

pH dependence of stability above pH 7

The decrease in stability with pH above 7, which is seen for *wt* barstar and H17Q, is characterized by an apparent pK_a of 9.2 ± 0.2 . Barstar has two free cysteine residues, both of which are buried (Lubienski et al., 1994). Thus, the pK_a values of these cysteines are expected to be higher than the intrinsic pK_a of the free cysteine residue (8.2), suggesting that the decrease in stability at high pH must be due to the deprotonation of either one or both of the sulfhydryl groups at high pH. The observation that there is no corresponding decrease in stability in the case of BSCCAA (Fig. 7B), where both the cysteine residues of barstar have been replaced by alanines, supports this argument. The pH dependence of C_m between pH 7 and 10 can be accounted for by Equation 9, in which only one group is assumed to be involved in the titration of the stability in this pH range. Moreover, the observed pH dependence of T_m (Fig. 8A,C) suggests that only one titratable group has deprotonated. Both these observations suggest that only one of the two cysteine residues is involved in the decrease in stability between pH 7 and 10. Currently, the pH dependence of the stability of each of the two mutants of barstar in which one or the other of the two cysteine residues has been mutated to alanine is being characterized in this laboratory in an effort to determine which of the two cysteines is responsible for this decrease in stability.

The ionization of any titratable group in a protein is linked to the $F \rightleftharpoons U$ unfolding reaction, and the change in the free energy of unfolding that occurs on titration depends on the difference in the pK_a value of that group in both the F and U states (Sali et al., 1988; Anderson et al., 1990). The apparent pK_a value reported here for any particular stability or unfolding transition depends on the values of the pK_a in both the F and U states, as well as on the free energy difference between the F and U states when both are deprotonated. A quantitative analysis of the effect of the change in pH on the free energy of unfolding has not been attempted here because the pK_a values of His 17 and the two Cys residues are not precisely known. There is an uncertainty in the precision of the measured apparent pK_a value of His 17 because its titration overlaps with that leading to the formation of the A form. A pH titration of the NMR chemical shifts of the ring protons of His 17 in *wt* barstar shows that His 17 does not even begin to titrate as the pH is lowered to 6 (S. Ramachandran & J.B. Udgaonkar, unpubl. results). Thus, the apparent pK_a value of His 17, estimated here to be 6.2 ± 0.2 , is probably substantially lower.

Three-state unfolding in the pH range 2–4

It has been shown previously (Khurana & Udgaonkar, 1994) that barstar adopts a molten globule-like conformation at pH values below 4. The noncoincidence of fluorescence-monitored and far-UV CD-monitored GdnHCl-induced denaturation curves that was characteristic of this conformation is also seen for BSCCAA below pH 5 (Fig. 7), indicating that BSCCAA also adopts a similar molten globule-like conformation below pH 4.

Three-state unfolding in the pH range 4–6

The observation that fluorescence-monitored unfolding precedes far-UV CD-monitored unfolding between pH 4 and 6 indicates that the fully folded protein F unfolds to U through an equilibrium intermediate I in this pH range. Thus, a three-state $F \rightleftharpoons I \rightleftharpoons U$ model is necessary to account for the equilibrium denaturation data. This decrease in stability from pH 7 to 5 has been attributed to the protonation of His 17 (see above). His 17 is buried in *wt* barstar, and a buried hydrogen bond exists between δN of His 17 and OH of Tyr 30. Because His 17 is buried, its pK_a value is expected to be lowered, and in fact its pK_a value has been determined here to be 6.2 compared to the value of 7.0 typically seen in unfolded proteins. The hydrogen bond must be disrupted before the His can be protonated, and hence protonation is expected to destabilize the protein. It has been shown that H17Q unfolds through a three-state mechanism at pH 7.0 (Nath & Udgaonkar, 1995), with the accumulation of at least one folding intermediate possessing a disrupted tertiary structure but retaining an intact secondary structure. The intermediate I observed for *wt* barstar and BSCCAA at pH 5 also has a more unstable tertiary structure than secondary structure (Fig. 7) and is probably similar to the intermediate seen with H17Q at pH 7.0. At present, the fluorescence and far-UV CD properties of I are unknown, and it is therefore not possible to carry out a detailed thermodynamic analysis according to the three-state model at pH 5 for *wt* barstar and for BSCCAA.

Two-state unfolding in the pH range 7–9

wt barstar shows two-state unfolding behavior in a very short range of pH between 7 and 9, where both the fluorescence-monitored and the CD-monitored unfolding curves superimpose exactly, giving identical values for C_m and ΔG_U . BSCCAA on the other hand exhibits two-state unfolding behavior from pH 6 to pH 10. The pH dependence of ΔG_U and C_m are similar for both *wt* barstar and BSCCAA, indicating that C_m is a good measure of stability for barstar.

Comparison of stability of wt barstar with both mutants BSCCAA and H17Q at pH 7

wt barstar is more stable than both BSCCAA and H17Q at pH 7. At pH 7, H17Q has been analyzed by a three-state model for unfolding and has been shown to have a ΔG_U of $3.6 \text{ kcal}\cdot\text{mol}^{-1}$ (Nath & Udgaonkar, 1995) compared to $5.0 \text{ kcal}\cdot\text{mol}^{-1}$ for *wt* barstar. The lower stability of H17Q over the *wt* has been attributed to the hydrogen bond between δN of His 17 and the -OH of the Tyr 30 of the *wt* barstar, which is not present in H17Q (Nath & Udgaonkar, 1995). BSCCAA is also less stable than *wt* barstar at pH 7–8 (Fig. 9). This lower stability is possibly because of the disruption of the hydrogen bond between the free -SH of Cys 40 residue and the carbonyl group of Ala 36 residue in the *wt* protein, which is not present in BSCCAA. The cysteines in *wt* barstar have been shown not to form a disulfide bond (S. Ramachandran & J.B. Udgaonkar, unpubl. results), and it has been shown that the two sulfhydryls in barstar are not close enough to form a disulfide bond (Lubienski et al., 1994). It should be noted that the structures and activities of BSCCAA and H17Q are similar to those of *wt* bar-

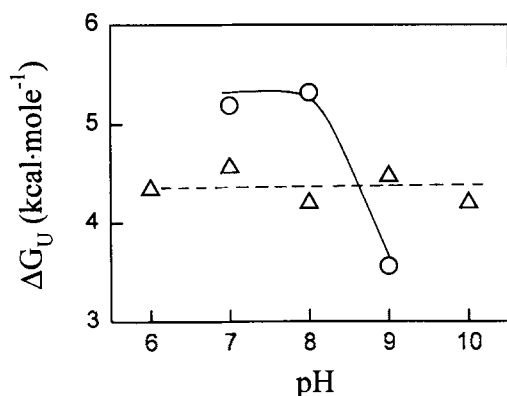


Fig. 9. pH dependence of $\Delta G_U(\text{H}_2\text{O})$ at 25 °C. ΔG_U values were obtained from GdnHCl-induced unfolding for wt barstar (○) and for BSCCAA (△) in the pH range where two-state unfolding transitions are exhibited. GdnHCl-induced denaturation curves were analyzed according to a two-state unfolding transition using Equations 1, 2, and 3. The value for $\Delta G_U(\text{H}_2\text{O})$ obtained from each curve is plotted against pH. Mean residue ellipticity at 220 nm and fluorescence at 322 nm were used as probes for unfolding. The solid line through the data for wt barstar and the dashed line through the data for BSCCAA were drawn by inspection only.

star (Guillet et al., 1993; Lubienski et al., 1994; Nath & Udgaonkar, 1995)

In summary, it has been shown here that the stability of barstar decreases when the pH is either reduced or raised from pH 7 by 2 pH units. In the former case the decrease is due to protonation of His 17, and in the latter case it is because of deprotonation of a Cys residue. Very high pH (>pH 12) completely unfolds the protein in a reversible manner. Very low pH (<pH 3) partially unfolds the protein in a reversible manner to a molten globule-like conformation that forms a large soluble oligomer.

Materials and methods

Materials

All chemicals were of the highest purity grade. Ultrapure urea was obtained from Research Organics Inc. and all other chemicals were obtained from Sigma Chemical Company.

Plasmids and protein purification

The plasmids encoding the genes for barstar (pMT316) and BSCCAA (pMT643) were a generous gift from Dr. R.W. Hartley (1988), and they were expressed in *Escherichia coli* strain MM294. The plasmid for the H17Q mutant of barstar was prepared by oligonucleotide-directed mutagenesis using PCR as described by Nath and Udgaonkar (1995). The procedure for the purification of barstar has been described previously (Khurana & Udgaonkar, 1994), and a similar procedure was used for purification of the mutant protein BSCCAA. The yield of pure BSCCAA was typically 50 mg/L for *E. coli* growth, compared to 200 mg/L for wt barstar. The method for purification of the H17Q mutant was also similar, except for the incorporation of an additional gel-filtration step using a Sephadex G-50 column; 2 mg of pure H17Q were obtained from 1 L of *E. coli* culture.

Buffers and solutions

The buffers that were used at different pH values were glycine (pH 2–3), sodium acetate (pH 4–5), sodium phosphate (pH 6–8), sodium borate (pH 9–10), and disodium hydrogen phosphate/sodium hydroxide (pH 11–12). All solutions used for equilibrium studies contained 20 mM buffer, 1 mM EDTA, and 1 mM DTT at pH 7. In all cases, buffer solutions were made by appropriate mixing of the acidic and basic forms of the buffer so as to obtain the desired final pH. For far-UV CD measurements, 200 μM DTT was used instead of 1 mM. The same buffers were used for temperature melts. The concentrations of the GdnHCl and urea stock solutions were determined by measurement of the refractive index (Pace et al., 1989). Urea solutions were prepared fresh on the day of use. All buffers were degassed before use.

Equilibrium unfolding studies

Equilibrium unfolding as a function of GdnHCl or urea concentration was monitored by fluorescence, far-UV CD, and near-UV CD. CD studies were done on a Jasco J720 spectropolarimeter. Spectra were collected with a slit width of 0.47 mm, response time of 1 s and scan speed of 20 nm/min. Each spectrum was the average of at least 10 scans. For denaturation studies, secondary structure was monitored at 220 nm and tertiary structure was monitored at 275 nm. Measurements were made with protein concentrations of 20 μM (far-UV) and 50 μM (near-UV) with cuvettes of pathlength 0.1 cm (far-UV) and 1 cm (near-UV).

Fluorescence studies were done using a Spex spectrofluorimeter. For studying intrinsic tryptophan fluorescence, the protein was excited at 287 nm and emission was monitored at 322 nm. The excitation slit width was set to 0.1 mm to avoid bleaching of the tryptophan fluorescence. All experiments were done at 25 °C. Measurements were made with a protein concentration of 4 μM or less, and a 1.0-cm-pathlength cuvette.

Thermal denaturation

Thermal denaturation was followed by monitoring absorbance at 287 nm in a Cary 1 spectrophotometer equipped with a Cary Peltier heating/cooling device, or by monitoring mean residue ellipticity at 220 nm (far-UV) and 275 nm (near-UV) using a Jasco J720 spectropolarimeter interfaced with a Neslab RTE-110 circulating bath. The heating rate used was 0.33 °C/minute. Using half this heating rate yielded an identical denaturation curve. The temperature in the cuvette was monitored during measurement using a Thermolyne digital pyrometer for the CD measurements and a Cary temperature probe for absorbance measurements. The accuracy of the probes was ± 0.5 °C.

Ultracentrifugation studies

Sedimentation equilibrium and sedimentation velocity measurements were made on a Beckman analytical ultracentrifuge model E using an AnHTi rotor with Schlieren optics. The protein concentrations used were 1 mM for both sedimentation equilibrium and sedimentation velocity experiments. A rotor speed of 68,000 rpm was used for the sedimentation velocity experiments. Sedimentation equilibrium experiments were performed and ana-

lyzed using the Archibald method. Sedimentation equilibrium measurements of the *A* form could not be carried out because of the nonavailability of a cell to perform a synthetic boundary experiment at low pH.

Gel-filtration studies

Size-exclusion chromatography of barstar at pH 3 in the presence of various concentrations of GdnHCl was carried out using a Superdex-75 column and a Pharmacia FPLC system. The concentration of protein used was typically 100 μ M.

Data analysis

Equilibrium unfolding data obtained using GdnHCl or urea as denaturants were converted to plots of f_U , the fraction of protein in the unfolded state, versus denaturant concentration using Equation 1:

$$f_U = \frac{Y_0 - (Y_F + m_F[D])}{(Y_U + m_U[D]) - (Y_F + m_F[D])}, \quad (1)$$

where Y_0 is the value of the spectroscopic property measured at a denaturant concentration $[D]$. Y_F and Y_U represent the intercepts, and m_F and m_U the slopes of the folded and unfolded baselines of the data, respectively, and are obtained from linear least-squares fits to the baselines.

For a two-state $F \rightleftharpoons U$ unfolding mechanism, ΔG_U , the free energy of unfolding by denaturant at concentration $[D]$ is related to f_U by a transformation of the Gibbs-Helmholtz equation in which the equilibrium constant for unfolding in the folding transition zone, K_{app} , is given by $K_{app} = f_U / (1 - f_U)$:

$$f_U = \frac{e^{-\frac{\Delta G_U}{RT}}}{1 + e^{-\frac{\Delta G_U}{RT}}}. \quad (2)$$

For denaturation by GdnHCl or urea, it is assumed that the free energy of unfolding, ΔG_U , has a linear dependence on the concentration of denaturant $[D]$ (Schellman, 1978):

$$\Delta G_U = \Delta G(\text{H}_2\text{O}) + m_G[D]. \quad (3)$$

$\Delta G_U(\text{H}_2\text{O})$ and m_G are therefore the intercept and the slope, respectively, of the plot of ΔG_U versus denaturant concentration. $\Delta G_U(\text{H}_2\text{O})$ corresponds to the free energy difference between the folded and unfolded states in the absence of any denaturant, and m_G is a measure of the cooperativity of the unfolding reaction. The concentration of denaturant at which the protein is half unfolded (when $\Delta G_U = 0$) is given by C_m , and from Equation 3, $\Delta G_U(\text{H}_2\text{O}) = -C_m m_G$.

For a two-state $F \rightleftharpoons U$ thermal unfolding transition, the free energy of unfolding, $\Delta G_U(T)$, at any temperature T is given by:

$$\Delta G_U(T) = \Delta H_m \left(1 - \frac{T}{T_m}\right) + \Delta C_p \left(T - T_m - T \ln \frac{T}{T_m}\right), \quad (4)$$

where T_m is the midpoint of the thermal transition, ΔH_m is the change in enthalpy that accompanies the $F \rightleftharpoons U$ unfolding reaction, and R is the gas constant (1.987 cal deg⁻¹ mol⁻¹). The basic assumption in Equation 4 is that ΔC_p , the change in heat capacity accompanying the $F \rightleftharpoons U$ unfolding reaction, is independent of temperature.

Thermal denaturation curves were analyzed as follows. The apparent equilibrium constant K_{app} and the free energy change ΔG_U at any temperature within the folding transition zone were first determined from the raw data using the following equations:

$$K_{app} = \frac{Y_0 - (Y_F + m_F T)}{(Y_U + m_U T) - Y_0} \quad (5)$$

$$\Delta G = -RT \ln K_{app} = -RT \ln \frac{Y_0 - (Y_F + m_F T)}{(Y_U + m_U T) - Y_0}, \quad (6)$$

where Y_0 is the spectroscopic property being measured at temperature T , and Y_F and Y_U represent the intercepts and m_F and m_U the slopes of the folded and unfolded baselines of the data, respectively. Values of K_{app} between 0.1 and 10 were used to make a plot of ΔG_U against T , and T_m was obtained as the temperature T at which $\Delta G_U = 0$. The slope of such a plot at T_m yielded ΔS_m , which from Equation 4 is equal to $-\Delta H_m / T_m$. Thus, ΔH_m could be determined. The value of ΔH_m was also obtained from the slope of a van't Hoff plot ($\ln K_{app}$ versus $1/T$), which is equal to $-\Delta H_m / R$. The two values for ΔH_m so obtained were essentially identical.

ΔC_p was obtained by assuming that ΔH is independent of GdnHCl concentration (Privalov, 1979). T_m was varied by varying the concentration of GdnHCl in the range 0–1.3 M, and ΔH_m was determined at each T_m . A linear least-squares fit of a plot of ΔH_m versus T_m yielded the slope as ΔC_p .

Thermal denaturation curves were therefore described, according to the two-state $F \rightleftharpoons U$ model for unfolding, by Equation 7:

$$Y_0(T) = \frac{(Y_F + m_F T) + (Y_U + m_U T) e^{\frac{\Delta H_m \left(\frac{T}{T_m} - 1\right) + \Delta C_p \left(T_m - T + T \ln \frac{T}{T_m}\right)}}{RT}}{1 + e^{\frac{\Delta H_m \left(\frac{T}{T_m} - 1\right) + \Delta C_p \left(T_m - T + T \ln \frac{T}{T_m}\right)}}{RT}}. \quad (7)$$

The numerator of the exponent in Equation 7 is equal to $-\Delta G_U(T)$, where $\Delta G_U(T)$ has been defined in Equation 4.

pH titrations

The structural unfolding transition observed at high pH was fitted to Equation 8, which is a transformation of the Henderson-Hasselbach equation:

$$Y = \frac{Y_D + Y_F 10^{\text{pH} - \text{pH}_{m1}}}{1 + 10^{\text{pH} - \text{pH}_{m1}}}. \quad (8)$$

In Equation 8, the structural unfolding transition has been associated with the titration of a single ionizable group. Y corresponds to the spectroscopic property at any pH, Y_D corresponds to the spectroscopic property for the denatured, deprotonated

(above pH 12) form, and Y_F is the optical property of the folded, protonated (pH 7–10) form. pH_{m1} corresponds to the midpoint of the pH transition and represents the apparent $\text{p}K_a$ that characterizes the high pH structural unfolding transition.

The C_m versus pH titration for *wt* barstar was fitted to Equation 9:

$$C_{obs} = \frac{C_F + C_{F^-} 10^{(\text{pH}-\text{pH}_{m2})} + \frac{C_{F^+}}{10^{(\text{pH}-\text{pH}_{m3})}} + \frac{C_A}{10^{(2\text{pH}-\text{pH}_{m3}-\text{pH}_{m4})}}}{1 + 10^{(\text{pH}-\text{pH}_{m2})} + \frac{1}{10^{(\text{pH}-\text{pH}_{m3})}} + \frac{1}{10^{(2\text{pH}-\text{pH}_{m3}-\text{pH}_{m4})}}} \quad (9)$$

In Equation 9, four forms of barstar are distinguished by different levels of protonation of three titratable groups that are important in determining stability. In the F^- form (above pH 10), none of the three titratable groups important in pH-dependent stability changes are protonated; in the F form, which exists at pH 7–8, one of these groups is protonated; in the F^+ form occurring at pH 5, one more group is also protonated; in the A form, which exists below pH 3, the third group is also protonated. C_{obs} is the observed C_m value at any pH, C_{F^-} is the C_m value for F^- form, C_F is the C_m value for the F form, C_{F^+} is the C_m value for the F^+ form and C_A is the C_m value for the A form. pH_{m2} is the midpoint of transition from the F^- form to the F form, pH_{m3} is the midpoint of transition from F form to F^+ form, and pH_{m4} is the midpoint of transition from the F^+ form to the A form. The three pH_m values correspond to the apparent $\text{p}K_a$ values that characterize these stability transitions.

The C_m versus pH titration for BSCCAA, in which the F to F^- form titration is not observed (Fig. 7B), was fit to Equation 10:

$$C_{obs} = \frac{C_F + \frac{C_{F^+}}{10^{(\text{pH}-\text{pH}_{m3})}} + \frac{C_A}{10^{(2\text{pH}-\text{pH}_{m3}-\text{pH}_{m4})}}}{1 + \frac{1}{10^{(\text{pH}-\text{pH}_{m3})}} + \frac{1}{10^{(2\text{pH}-\text{pH}_{m3}-\text{pH}_{m4})}}} \quad (10)$$

The C_m versus pH plot for H17Q, in which the F^+ form is not observed at pH 5 (Fig. 7C), has been fit to Equation 11:

$$C_{obs} = \frac{C_F + C_{F^-} 10^{(\text{pH}-\text{pH}_{m2})} + \frac{C_A}{10^{(\text{pH}-\text{pH}_{m4})}}}{1 + 10^{(\text{pH}-\text{pH}_{m2})} + \frac{1}{10^{(\text{pH}-\text{pH}_{m4})}}} \quad (11)$$

In Equation 11, pH_{m4} is the apparent $\text{p}K_a$ that describes the transition from the F to the A state.

The number of protons that are released from or bind to a protein on a change in pH is given by Equation 12 (Ptitsyn & Birshtein, 1969):

$$\Delta_m \nu = - \frac{\Delta H_m(T_m)}{2.303 RT_m^2} \frac{dT_m}{d\text{pH}}, \quad (12)$$

where T_m is the midpoint of a thermally induced unfolding transition at a particular pH, ΔH_m is the enthalpy determined

by the van't Hoff method at T_m , and $dT_m/d\text{pH}$ is the pH dependence of T_m at that particular pH.

Acknowledgments

We thank V. Agashe for his comments on the manuscript and Dr. T.R.K. Murti for his help with ultracentrifugation studies done at CCMB, Hyderabad. This work was funded by the Tata Institute of Fundamental Research, and by the Department of Biotechnology, Government of India. J.B.U. is the recipient of a Biotechnology Career Fellowship from the Rockefeller Foundation.

References

- Alexandrescu AT, Evans PA, Pitkeathly M, Baum J, Dobson CM. 1993. Structure and dynamics of the acid-denatured molten globule state of α -lactalbumin: A two-dimensional NMR study. *Biochemistry* 32:1707–1718.
- Anderson DE, Becktel WJ, Dahlquist FW. 1990. pH-induced denaturation of proteins: A single salt bridge contributes 3–5 kcal/mol to the free energy of folding of T4 lysozyme. *Biochemistry* 29:2403–2408.
- Beychok S, Steinhardt J. 1959. Increase in acid-binding sites on denaturation of horse ferrihemoglobin at 0 °C. *J Am Chem Soc* 81:5679–56.
- Burger HG, Edelhock H, Condliffe PG. 1966. The properties of bovine growth hormone 1. Behavior in acid solutions. *J Biol Chem* 241:449–457.
- Bychkova VE, Berni R, Rossi GL, Kutysenko VP, Ptitsyn OB. 1992. Retinol-binding protein is in the molten globule state at low pH. *Biochemistry* 31:7566–7571.
- Cavard D, Sauve P, Heitz F, Pattus F, Martinez C, Dijkman R, Lazdunski C. 1988. Hydrodynamic properties of colicin A: Existence of a high-affinity lipid binding site and oligomerization at acid pH. *Eur J Biochem* 172:507–512.
- Chen YH, Yang JT, Martinez HM. 1972. Determination of the secondary structure of proteins by circular dichroism and optical rotatory dispersion. *Biochemistry* 11:4120–4131.
- Dolgikh DA, Abaturav LV, Brazhnikov EV, Lebedev YuO, Chirgadze YuN, Ptitsyn OB. 1983. Acid form of carbonic anhydrase: “Molten globule” with a secondary structure. *Dokl Akad Nauk SSSR* 272:1481–1484.
- Dolgikh DA, Gilmanshin EV, Brazhnikov V, Bychkova VE, Semisotnov GV, Venyaminov SYu, Ptitsyn OB. 1981. α -Lactalbumin: Compact state with fluctuating tertiary structure? *FEBS Lett* 136:311–315.
- Eftink MR, Helton KJ, Beavers A, Ramsay GD. 1994. The unfolding of trp aporepressor as a function of pH: Evidence for an unfolding intermediate. *Biochemistry* 33:10220–10228.
- Fink AL, Calciano LJ, Goto Y, Kurotsu T, Palleros DR. 1994. Classification of acid denaturation of proteins: Intermediates and unfolded states. *Biochemistry* 33:12504–12511.
- Goto Y, Calciano LJ, Fink AL. 1990. Acid induced folding of proteins. *Proc Natl Acad Sci USA* 87:573–577.
- Goto Y, Fink AL. 1989. Conformational states of β -lactamase: Molten-globule states at acidic and alkaline pH with high salt. *Biochemistry* 28:945–952.
- Griko YuV, Privalov PL, Venyaminov SYu, Kutysenko VP. 1988. Thermodynamic study of apomyoglobin structure. *J Mol Biol* 202:127–138.
- Guillet V, Laphorn A, Hartley RW, Mauguen Y. 1993. Recognition between a bacterial ribonuclease barnase, and its natural inhibitor, barstar. *Structure* 1:165–176.
- Hartley RW. 1988. Barnase and barstar. Expression of its cloned inhibitor permits expression of a cloned ribonuclease. *J Mol Biol* 202:913–915.
- Hermans J, Scheraga HA. 1961. Structural studies of ribonuclease. V. Reversible change of configuration. *J Am Chem Soc* 83:3283–3292.
- Herold M, Kirchner K. 1990. Reversible dissociation and unfolding of aspartate aminotransferase from *E. coli*: Characterization of a monomeric intermediate. *Biochemistry* 29:1907–1913.
- Khurana R, Udgaonkar JB. 1994. Equilibrium unfolding studies of barstar: Evidence for an alternative conformation which resembles a molten globule. *Biochemistry* 33:106–115.
- Kuwajima K. 1992. Protein folding in vitro. *Curr Opin Biotechnol* 3:462–467.
- Linderström-Lang K. 1924. *CR Trav Lab Carlsberg* 15–70.
- Lubienski MJ, Bycroft M, Freund SMV, Fersht AR. 1994. Three-dimensional solution structure and ^{13}C assignments of barstar using nuclear magnetic resonance spectroscopy. *Biochemistry* 33:8866–8877.
- McPhie P. 1975. pH dependence of the thermal unfolding of ribonuclease A. *Biochemistry* 11:879–883.
- Nath U, Udgaonkar JB. 1995. Perturbation of a tertiary hydrogen bond in barstar by mutagenesis of the sole His residue to Gln leads to accumu-

- lation of at least one equilibrium folding intermediate. *Biochemistry* 34:1702-1713.
- Ohgushi M, Wada A. 1983. "Molten-globule state": A compact form of globular proteins with mobile side chains. *FEBS Lett* 164:21-24.
- Pace CN, Laurens DV. 1989. A new method for determining the heat capacity change for protein unfolding. *Biochemistry* 28:2520-2525.
- Pace CN, Laurens DV, Erikson RE. 1992. Urea denaturation of barnase: pH dependence and characterization of the unfolded state. *Biochemistry* 31:2728-2734.
- Pace CN, Laurens DV, Thomson JA. 1990. pH dependence of the urea and guanidine hydrochloride denaturation of ribonuclease A and ribonuclease T1. *Biochemistry* 29:2564-2572.
- Pace CN, Shirely BA, Thomson JA. 1989. Measurement of conformational stability of a protein. In: Creighton TE, ed. *Protein structure: A practical approach*. Oxford, UK: IRL Press. pp 311-330.
- Privalov PL. 1979. Stability of proteins: Small globular proteins. *Adv Protein Chem* 33:167-241.
- Ptitsyn OB, Birshtein TM. 1969. Method of determining the relative stability of different conformational states of biological macromolecules. *Biopolymers* 7:435-445.
- Redfield C, Smith RAG, Dobson CM. 1994. Structural characterization of a highly-ordered "molten-globule" at low pH. *Nature Struct Biol* 1:23-29.
- Robbins FM, Holmes LG. 1970. Circular dichroism spectra of α -lactalbumin. *Biochim Biophys Acta* 221:234-240.
- Sali D, Bycroft M, Fersht AR. 1988. Stabilization of protein structure by interaction of an α -helix dipole with a charged side chain. *Nature* 335:740-743.
- Schellman JA. 1978. Solvent denaturation. *Biopolymers* 7:1305-1322.
- Schreiber G, Fersht AR. 1993a. The refolding of *cis*- and *trans*-peptidyl prolyl isomers of barstar. *Biochemistry* 32:11195-11203.
- Schreiber G, Fersht AR. 1993b. Interaction of barnase with its polypeptide inhibitor barstar studied by protein engineering. *Biochemistry* 32:5145-5150.
- Shastri MCR, Agashe VR, Udgaonkar JB. 1994. Quantitative analysis of the kinetics of denaturation and renaturation of barstar in the folding transition zone. *Protein Sci* 3:1409-1417.
- Shastri MCR, Udgaonkar JB. 1995. The folding pathway of barstar: Evidence for multiple pathways and multiple intermediates. *J Mol Biol* 247:1013-1027.
- Swaminathan R, Periasamy N, Udgaonkar JB, Krishnamoorthy G. 1994. Molten globule-like conformation of barstar: A study by fluorescence dynamics. *J Phys Chem* 98:9270-9278.
- Tanford C. 1970. Protein denaturation (part C). *Adv Protein Chem* 24:1-95.